YALE
PEABODY
MUSEUM

P.O. BOX 208118 | NEW HAVEN CT 06520-8118 USA | PEABODY.YALE. EDU

JOURNAL OF MARINE RESEARCH

The *Journal of Marine Research,* one of the oldest journals in American marine science, published important peer-reviewed original research on a broad array of topics in physical, biological, and chemical oceanography vital to the academic oceanographic community in the long and rich tradition of the Sears Foundation for Marine Research at Yale University.

An archive of all issues from 1937 to 2021 (Volume 1–79) are available through EliScholar, a digital platform for scholarly publishing provided by Yale University Library at https://elischolar.library.yale.edu/.

Requests for permission to clear rights for use of this content should be directed to the authors, their estates, or other representatives. The *Journal of Marine Research* has no contact information beyond the affiliations listed in the published articles. We ask that you provide attribution to the *Journal of Marine Research*.

Yale University provides access to these materials for educational and research purposes only. Copyright or other proprietary rights to content contained in this document may be held by individuals or entities other than, or in addition to, Yale University. You are solely responsible for determining the ownership of the copyright, and for obtaining permission for your intended use. Yale University makes no warranty that your distribution, reproduction, or other use of these materials will not infringe the rights of third parties.

This work is licensed under a Creative Commons Attribution-NonCommercial-ShareAlike 4.0 International License.
https://creativecommons.org/licenses/by-nc-sa/4.0/

Journal of Marine Research, 52, 999–1016, 1994

A proposed flux constraint for salt fingers in shear

by Eric Kunze[1]

ABSTRACT

Towed ocean microstructure observations reveal that the temperature Cox number depends inversely on interface temperature-gradient $\overline{T}_z$ in the fingering-favorable thermohaline staircase east of Barbados. This implies fluxes independent of interface gradients. These conclusions are contrary to theoretical expectations from a finger Froude number stability criterion, $|\nabla w|/N < 1.0$: (i) Cox numbers independent of temperature gradient, and (ii) fluxes varying linearly with temperature gradient. We propose a hybrid wave/finger Froude number stability criterion, $|(u_z - w_x)(w_y - v_z)|N^2 \leq 1.0$ which reduces to $U_z|\nabla w|/N^2 \leq 1.0$ for salt sheets ($\partial/\partial x = 0, |\nabla w| = w_y$) aligned with background (internal-wave) shear U_z. The sheet criterion reproduces the observed behavior. For weak but nonzero background shears, $0.1 < U_z/N < 1.0$, this constraint implies higher fluxes than unsheared square-planform fingers constrained by a finger Froude number $|w_x w_y|/N^2 < 1.0$.

1. Introduction

Microstructure measurements collected in the thermohaline staircase east of Barbados during the 1985 C-SALT experiment (Schmitt *et al.,* 1987) dramatically advanced our understanding of salt fingers' role in ocean mixing, revising estimates of their fluxes downward to levels comparable to shear-driven turbulence (Gregg, 1989; Ledwell *et al.,* 1993). Previous work (Lambert and Sturges, 1977; Schmitt, 1981; Gargett and Schmitt, 1982) based on laboratory $\Delta S^{4/3}$ flux laws (Turner, 1967; Linden, 1973; Schmitt, 1979) had suggested that fingering fluxes could completely dominate water-mass modification in Central Waters. In C-SALT, the fluxes were found to be a factor of 30 below laboratory predictions (Gregg and Sanford, 1987; Lueck, 1987). This was argued (Kunze, 1987) to arise because ocean interfaces are much thicker than the predicted maximum finger height h_{max} based on a finger Froude number $Fr_f = |\nabla w|/N \leq 1.0$ or Stern (1969, 1975) number $A = \langle wb \rangle / \nu N^2 \leq 1.0$ constraint where the buoyancy $b = -g\delta\rho/\rho$; in two-layer laboratory experiments, the interface thickness is set by the maximum finger height ($l_i = h_{max}$).

Optical shadowgraph profiles in the staircase (Kunze *et al.,* 1987) found 0.5-cm thick, nearly horizontal laminae in the fingering-favorable parts of the water column rather than the 3-cm vertical banding expected for salt fingers. To explain this, Kunze

1. School of Oceanography WB-10, University of Washington, Seattle, Washington, 98195, U.S.A.

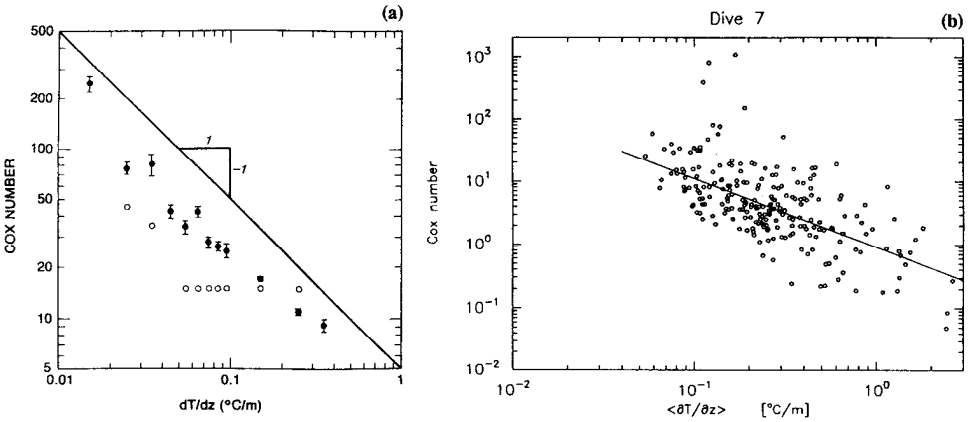

Figure 1. Temperature Cox number C_T versus vertical temperature-gradient $\overline{T}_z$ in interfaces of the thermohaline staircase east of Barbados from (a) a towed microscale conductivity cell (after Marmorino, 1989) and (b) a towed microthermistor (after Fleury and Lueck, 1991). The solid dots in (a) denote the mean of the distribution, the open circles the mode. Only the means are displayed in (b). Both data sets have mean Cox numbers $C_T \alpha \overline{T}_z^{-1}$. Theory (Kunze, 1987) predicts a Cox number of ~8, independent of temperature-gradient.

(1990) developed a model for the behavior of salt sheets in near-inertial shear. Initially aligned with the shear U_z ($k_x = 0$), the sheets are slowly tilted as the inertial shear turns out of alignment. But the sheets should be disrupted by instability processes ($Fr_f > 1.0$) before tilting more than 40°. The small scale of the laminae indicates that they must be entirely due to salt (Kunze *et al.*, 1987). It appears that they are salt remnants left behind by disrupted fingers that have been slowly sheared out.

As yet unexplained, towed microstructure measurements during C-SALT (Marmorino, 1989; Fleury and Lueck, 1991) found an inverse dependence of temperature Cox number C_T on temperature gradient $\overline{T}_z$ (Fig. 1). This inverse dependence is more obvious in the mean than the mode (o, Fig. 1a). It corresponds to a linear dependence on interface thickness l_i for fixed temperature step ΔT. It contradicts the finger Froude number constraint which predicts temperature Cox numbers independent of $\overline{T}_z$ and l_i (Kunze, 1987). In this paper, we will seek a nondimensional constraint on finger growth that will reproduce the observed Cox number's dependence on interface thickness and explore the consequences of such a constraint for oceanic salt-finger fluxes.

2. The Cox number

Following Kunze (1987), the temperature Cox number for growing salt fingers can be expressed in terms of the finger height h

$$C_T = \frac{(\nabla T)^2}{\overline{T}_z^2} \simeq \frac{k^2 \delta T^2}{\overline{T}_z^2} = \frac{k^2 \delta_T^2 h^2}{4} \tag{1}$$

where k is the wavenumber, $\overline{T}_z$ the background interface temperature gradient, δT the finger-induced temperature anomaly and $\delta_T = 2\delta T/(\overline{T}_z h)$ its nondimensional form. This ignores gradients at the finger tips which should augment the finger Cox number by no more than 10% for typical finger aspect ratios. The reader is referred to Kunze (1987) for the equations of motion and a more complete discussion of salt-fingering physics. Because inertial shear tilting does not appear to dramatically alter fingering fluxes (Kunze, 1990) and for analytic tractability, we will assume fastest-growing fingers as found in the lab (Turner, 1967; Schmitt, 1979; Taylor and Bucens, 1989). The nondimensional temperature anomaly for fastest-growing fingers

$$\delta_T = \frac{\sqrt{R_\rho} - \sqrt{R_\rho - 1}}{2\sqrt{R_\rho}} \tag{2}$$

is a function only of density ratio $R_\rho = \alpha\overline{T}_z/\beta\overline{S}_z$ (= 1.6 in C-SALT, Schmitt *et al.*, 1987). The fastest-growing wavenumber obeys

$$k^2 = \frac{N}{\sqrt{\nu\kappa_T}} = \sqrt{\frac{g\beta\overline{S}_z(R_\rho - 1)}{\nu\kappa_T}} = \sqrt{\frac{g\beta\Delta S(R_\rho - 1)}{\nu\kappa_T l_i}} \tag{3}$$

where l_i is the interface thickness and ΔS (= 0.09 ‰ in C-SALT, Boyd and Perkins, 1987) the salinity step across the interface. Substituting (2) and (3) into (1), the temperature Cox number becomes

$$C_T = \frac{\sqrt{g\beta\Delta S}h^2}{16\sqrt{\nu\kappa_T l_i}} \frac{\sqrt{R_\rho - 1}(\sqrt{R_\rho} - \sqrt{R_\rho - 1})^2}{R_\rho} \alpha \frac{h^2}{l_i^{1/2}}. \tag{4}$$

Therefore, for the temperature Cox number to be proportional to interface thickness l_i, as observed in the C-SALT staircase interfaces by Marmorino (1989) and Fleury and Lueck (1991), the finger height

$$\boxed{h \alpha l_i^{3/4}.} \tag{5}$$

In contrast, the finger Froude number ($|\nabla w|/N \leq 1.0$; Kunze, 1987) and Stern (1969, 1975) number ($\langle wb\rangle/\nu N^2 \leq 1.0$) constraints predict finger heights $h \alpha l_i^{1/4}$ and Cox numbers independent of interface thickness. These two constraints are equivalent for high Prandtl number ν/κ_T fluids where the vertical accleration $\partial w/\partial t$ can be neglected. Clearly, neither describe the observed Cox number's variation with interface thickness in the thermohaline staircase east of Barbados, although they appear to predict both laboratory fluxes and *mean* ocean Cox numbers reasonably well (Kunze, 1987; Fleury and Lueck, 1991).

One factor which might influence the stability of growing fingers in the ocean that is absent from most laboratory experiments is background shear. Velocity profiles collected in C-SALT by Gregg and Sanford (1987) found weak but significant near-inertial shear across the interfaces (1-m $Ri_w = 6$ on average). In the laboratory,

Linden (1974) showed that sheared fingers form vertical sheets aligned with mean shear U_z of horizontal planform $\sin(k_y y)$ rather than the square planform $\sin(k_x x)\sin(k_y y)$ characterizing unsheared conditions (Shirtcliffe and Turner, 1970). Kunze (1990) suggested that similar aligned sheets would form in inertial shear but would be slowly tilted as the shear turned out of alignment with them. This appears to occur slowly enough that the sheets are only slightly tilted and their fluxes only slightly modified before being disrupted by instability so shear tilting will be ignored here.

The velocity profiles collected by Gregg and Sanford (Fig. 2a) reveal that the velocity step across the interfaces is independent of interface thickness ($\Delta U = 1.4 \pm 0.1$ cm s^{-1}). This implies that the wave-induced Froude number $|\mathbf{V}_z|/N = \Delta U/\sqrt{g\beta\Delta S l_i(R_\rho - 1)}\alpha l_i^{-1/2}$ is larger across thinner interfaces (Fig. 2b). This is in the right sense to disrupt fingers earlier during their growth, producing smaller Cox numbers in thinner interfaces as observed in C-SALT. To explore this possibility more quantitatively, we will seek an $\sim$O(1) nondimensional constraint involving the background shear U_z and finger height h which reproduces a temperature Cox number $C_T \alpha\, l_i$. We will do this by examining ratios of the timescales in the sheared salt-finger problem.

3. Timescales

There are three timescales associated with stabilizing agents and three associated with potentially destabilizing processes for salt fingers growing in a background shear U_z. As with the Cox number, these can be expressed in terms of the finger height h and interface thickness l_i for fastest-growing fingers following Kunze (1987).

Stabilizing timescales are

(i) the buoyancy frequency $N = \sqrt{g\beta\overline{S}_z(R_\rho - 1)} = \sqrt{\dfrac{g\beta\Delta S(R_\rho - 1)}{l_i}}$ (6)

(ii) viscous damping $\nu k^2 = N\sqrt{\dfrac{\nu}{\kappa_T}} = \sqrt{\dfrac{\nu g\beta\Delta S(R_\rho - 1)}{\kappa_T l_i}}$ (7)

from (3); diffusive timescales involving κ_T and κ_S are similar in form. Viscous damping is larger than the buoyancy frequency N by the square root Prandtl number $\sqrt{\nu/\kappa_T} \simeq 3$.

(iii) finger growth rate $\sigma = \dfrac{1}{2}\sqrt{\dfrac{(\kappa_T - R_\rho\kappa_S)g\beta\Delta S}{\nu l_i}}(\sqrt{R_\rho} - \sqrt{R_\rho - 1})$. (8)

This can be argued to be a 'stabilizing' timescale in the sense that, if the disrupting instability does not grow faster than the fingers themselves, it is unlikely to be important. The finger growth rate $\sigma < N < \nu k^2$ (Kunze, 1987). All three stabilizing timescales are proportional to $l_i^{-1/2}$ so are indistinguishable for our purposes. We will

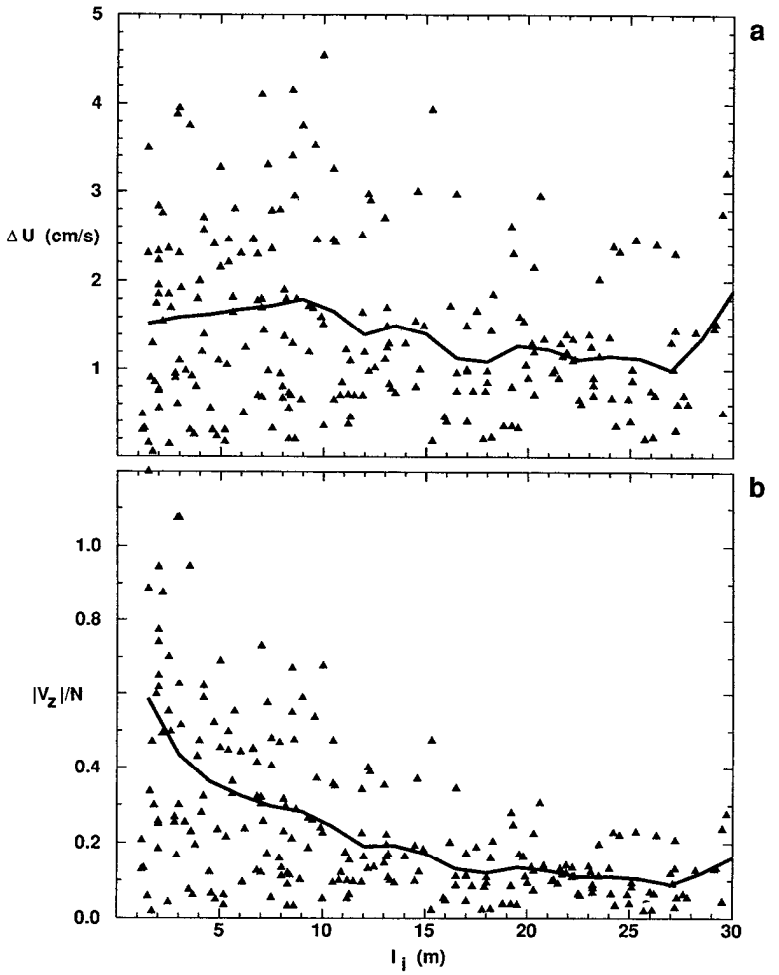

Figure 2. (a) Velocity steps ΔU (a) and Froude numbers $|\mathbf{V}_z|/N = \Delta U/\sqrt{g\beta\Delta S(R_\rho - 1)l_i}$ (b) as a function of interface thickness l_i across the steps in the thermohaline staircase east of Barbados. Triangles denote individual estimates and the curves averages over 2-m l_i bins. On average, the velocity difference is 1.4 cm s^{-1}, independent of interface thickness. The Froude number is significantly larger across thinner interfaces, but remains below the critical value of 1.0 provided $l_i > 0.5$ m.

use the buoyancy frequency N because it is a true external parameter, independent of assumptions about the fingering physics.

Destabilizing timescales are

(iv) the background near-inertial shear $|\mathbf{V}_z| = U_z = \dfrac{\Delta U}{l_i} \alpha \dfrac{1}{l_i}$ (9)

where this inverse dependence on interface thickness l_i arises because the velocity step ΔU is independent of interface thickness in the staircase east of Barbados (Fig. 2a),

(v) the finger shear

$$|\nabla w| \simeq kw = \frac{\sigma k h}{2}$$

$$= \frac{\kappa_T^{1/4}(g\beta\Delta S)^{3/4}}{\nu^{3/4}} \frac{h}{l_i^{3/4}} (R_\rho - 1)^{1/4}(\sqrt{R_\rho - \sqrt{R_\rho - 1}}) \, \alpha \, \frac{h}{l_i^{3/4}} \tag{10}$$

where $w = \sigma h/2$ for exponentially-growing fingers (Kunze, 1987) and σ is the finger growth rate (8), and

(vi) the buoyancy-gradient anomaly at the finger's tip

$$\sqrt{\nabla b} = \sqrt{\nu k^3 w} = \frac{(g\beta\Delta S)^{5/8}}{2(\nu\kappa_T)^{1/8}} \frac{h^{1/2}}{l_i^{5/8}} \frac{\sqrt{\sqrt{R_\rho} - \sqrt{R_\rho - 1}}}{(R_\rho - 1)^{1/4}} \, \alpha \, \frac{h^{1/2}}{l_i^{5/8}} \tag{11}$$

using $b = \nu\nabla^2 w$ from the vertical momentum equation (Kunze, 1987), where the buoyancy anomaly $b = -g\delta\rho/\rho_o$, and it has been assumed that the finger tip's vertical scale is identical to the fastest-growing wavenumber k.

Finger growth and fluxes will be disrupted when destabilizing effects overcome stabilizing. We seek a nondimensional ratio of destabilizing to stabilizing timescales that produces $h \, \alpha \, l_i^{3/4}$ (5). Previous guesses for the nondimensional parameter constraining finger growth include the finger Froude number (Richardson number)

$$Fr_f \equiv Ri_f^{-1/2} = \frac{|\nabla w|}{N} = \frac{(\kappa_T g\beta\Delta S)^{1/4} h}{4\nu^{3/4} l_i^{1/4}} \frac{\sqrt{R_\rho} - \sqrt{R_\rho - 1}}{(R_\rho - 1)^{1/4}} \, \alpha \, \frac{h}{l_i^{1/4}} \tag{12}$$

(Kunze, 1987), the Stern (1969; 1975) number

$$\frac{\langle wb \rangle}{\nu N^2} = \frac{k^2 w^2}{N^2} \, \alpha \, \frac{h^2}{l_i^{1/2}}, \tag{13}$$

where $\langle wb \rangle$ is the finger-induced buoyancy-flux, and the finger Reynolds number

$$\frac{|\nabla w|}{\nu k^2} = \frac{kw}{N} \sqrt{\frac{\kappa_T}{\nu}} \, \alpha \, \frac{h^2}{l_i^{1/2}} \tag{14}$$

all of which imply $h \, \alpha \, l_i^{1/4}$ and a Cox number independent of interface thickness l_i, contrary to the C-SALT measurements.

A nondimensional parameter which displays the desired dependence between h and l_i is the ratio of the background shear U_z (9) times the finger shear ∇w (10)

divided by the buoyancy frequency squared N^2 (6),

$$\boxed{\frac{|U_z \nabla w|}{N^2} = \frac{\kappa_T^{1/4} \Delta U}{4\nu^{3/4}(g\beta\Delta S)^{1/4}} \frac{h}{l_i^{3/4}} \frac{(\sqrt{R_\rho} - \sqrt{R_\rho - 1})}{(R_\rho - 1)^{3/4}} \alpha \frac{h}{l_i^{3/4}}} \tag{15}$$

where the denominator could be replaced by $\nu^2 k^4$, $\nu k^2 N$, etc., for the same dependence on h and l_i. We will refer to this parameter as the *hybrid wave/finger Froude number* $Fr_{w/f} = Fr_w Fr_f$ where the background Froude number $Fr_w = |\mathbf{V}_z|/N = U_z/N$ is dominated by finescale near-inertial waves in the ocean. For $U_z/N < 1.0$, the hybrid wave/finger Froude number constraint (15) will permit larger finger amplitudes and fluxes for shear-aligned sheets ($k_x = w_x = 0$) than the finger Froude number constraint (12) does for square planform fingers ($k_x = k_y$, $w_x = w_y$) because the background shear suppresses the alongshear w_x (Linden, 1974).

The above nondimensional number might be generalized as the product of the two horizontal vorticity components normalized by the stratification

$$\boxed{Fr_{w/f} = \frac{|(w_y - v_z)(u_z - w_x)|}{N^2} \leq Fr_c^2.} \tag{16}$$

This constraint would be more appropriate than (15) when the background shear U_z is too weak to suppress square planform fingers in favor of shear-aligned sheets. Constraint (16) follows by recognizing that, when horizontal vortices are strong enough, they can overcome stratification to transform horizontal vorticity into vertical and produce isotropic three-dimensional turbulence. This turbulence will disrupt the finger fluxes (Linden, 1971). Generalization (16) reduces (apart from a factor of two which is within measurement errors) to the finger Froude number condition (Kunze, 1987) for square planform fingers ($k_x = k_y = k/\sqrt{2}$) in the absence of background shear ($U_z/N \ll 1.0$)

$$Fr_f^2 = \frac{|w_x w_y|}{N^2} = \frac{|k_x k_y| w^2}{N^2} = \frac{k^2 w^2}{2N^2} \leq Fr_c^2. \tag{17}$$

4. Comparison with ocean measurements

To test constraint (15) against the data, we substitute it into (4) to obtain the maximum Cox number for salt sheets in a background shear

$$\max C_T = \frac{Fr_c^2 \cdot \nu g\beta\Delta S \cdot l_i(R_\rho - 1)}{\kappa_T \Delta U^2 R_\rho}. \tag{18}$$

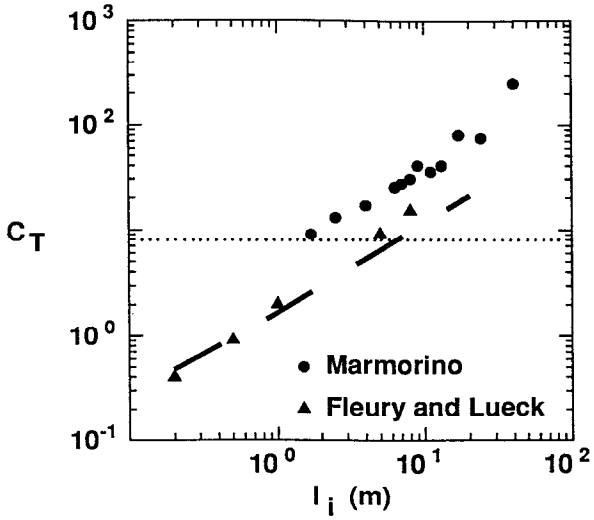

Figure 3. Comparison of the observed temperature Cox number's C_T dependence on interface thickness l_i (▲, ●) with the model prediction for a critical $Fr_{w/f} = (U_z w_y)/N^2 = 1.0$ (15) constraint (dashed line). The unsheared square planform fingers prediction of ~8 is independent of interface thickness (Kunze, 1987). The predicted Cox number C_T has the same linear dependence on interface thickness l_i as the observations. The predicted level is consistent with Fleury and Lueck (1991) for $Fr_c = 1.0$. Marmorino's (1989) values are a factor of three higher and are well-reproduced for $Fr_c = 2.0$ (see text).

The average model temperature Cox number is then (18) normalized by the time integral from finger inception to disruption by instability, e.g.,

$$\langle C_T \rangle = \left(\frac{1}{2\sigma t_{\max}} \right) \frac{Fr_c^2 \cdot vg\beta\Delta S \cdot l_i (R_\rho - 1)}{\kappa_T \Delta U^2 R_\rho} \tag{19}$$

where the normalization factor corrected from Kunze (1987)

$$2\sigma t_{\max} = 2\ln (kh_{\max}) = \ln \left[\frac{16\, Fr_c^2 vg\beta\Delta S l_i}{\kappa_T \Delta U^2} \frac{(R_\rho - 1)^2}{(\sqrt{R_\rho} - \sqrt{R_\rho - 1})^2} \right] \tag{20}$$

arises from (3) and (15). Figure 3 compares the dependence on interface thickness l_i of the average model temperature Cox number (19) (dashed) for a critical hybrid wave/finger Froude number $Fr_c = 1.0$, velocity step $\Delta U = 1.4$ cm s^{-1}, density ratio $R_\rho = 1.6$ and salinity step $\Delta S = 0.09$ ‰ (consistent with the C-SALT interfaces, Boyd and Perkins, 1987) with the microstructure observations (triangles and dots). The hybrid constraint reproduces the Fleury and Lueck (1991) observations. The Marmorino (1989) values are higher by a factor of three, have a slightly gentler slope and are well-reproduced with $Fr_c = 2.0$. The discrepancy between the two microstructure measurements was not discussed by Fleury and Lueck (1991). It may be due to

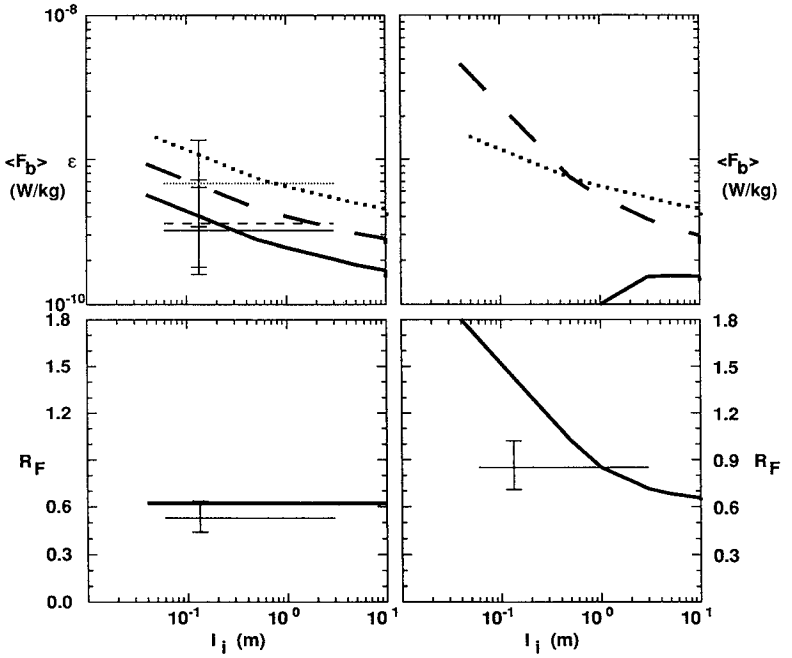

Figure 4. The dependence on interface thickness l_i of the model's average buoyancy - ($\langle F_b \rangle = \epsilon$, thick solid), heat - ($g\alpha\langle F_T \rangle$, thick dashed) and salt-fluxes ($g\beta\langle F_S \rangle$, thick dotted) [upper panels]; and flux ratio $R_F = \alpha\langle F_T \rangle / \beta\langle F_S \rangle$ [lower panels] for a critical $Fr_{w/f} = 1.0$. Also shown are observed magnitudes (thin horizontal lines) along with their error bars. The left panels display finger values only, the right panels include molecular diffusion.

(i) higher horizontal resolution of the microscale conductivity cell employed by Marmorino, (ii) contamination by high-wavenumber salinity microstructure in that signal, (iii) coarser vertical resolution in his measurements (1 m compared to 0.4 m), or (iv) differing definitions of Cox number used by the two investigators. Temperature and conductivity Cox numbers are identical for fingers at a density ratio $R_\rho = 1.6$. However, for salinity-gradient variance to be dissipated, salinity microscales $\sqrt{\kappa_S/\kappa_T} = 0.1$ smaller than temperature microscales must be produced. This would imply conductivity Cox numbers $C_\sigma = 19C_T$ but the salinity microscale was not fully resolved by Marmorino's sensor.

Figure 4 compares model fluxes and flux ratios with estimates inferred from Fleury and Lueck (1991). Their Table 3 quotes values for the heat-flux F_T, flux ratio R_F and layer dissipation rates ϵ, from which we infer the buoyancy-flux F_b ($= \epsilon$) and salt-flux $g\beta F_S (= g\alpha F_T/R_F)$. The model reproduces the fluxes (dissipation rates) with at most a factor of two in variability associated with factor of 100 variability in interface thicknesses and gradients. Levels are comparable. In particular, constraint (15) correctly predicts fluxes substantially below $\Delta S^{4/3}$ law fluxes under conditions when the interface thickness $l_i = h_{\max}$ and Kunze (1987) predicts $\Delta S^{4/3}$ fluxes.

5. Comparison with laboratory measurements

Linden (1974) explored the sensitivity of salt fingers in sheared two-layer experiments. He reported a tendency for the salt-flux to increase and the interface to thin as the shear ΔU increased. If we assume as in Kunze (1987), that the interface thickness is equal to the maximum finger height in two-layer laboratory experiments ($l_i = h_{\max}$), then the hybrid wave/finger Froude number (15) for shear-aligned sheets ($k_x = 0$) can be written

$$Fr_{w/f} = \frac{\Delta U \kappa_T^{1/4}(\sqrt{R_\rho} - \sqrt{R_\rho - 1})h^{1/4}}{4\nu^{3/4}(g\beta\Delta S)^{1/4}(R_\rho - 1)^{3/4}} \leq Fr_c \tag{21}$$

where ΔU and ΔS are the velocity and salinity steps across the interface as before. From (21), the interface thickness and maximum finger height

$$l_i = h_{\max} = \frac{256 Fr_c^4 \nu^3 g\beta\Delta S(R_\rho - 1)^3}{\kappa_T \Delta U^4(\sqrt{R_\rho} - \sqrt{R_\rho - 1})^4}, \tag{22}$$

which thins with increasing velocity step ΔU but is extremely sensitive to ΔU and critical Froude number Fr_c. The resulting interfacial Froude number

$$\frac{U_z}{N} = \frac{\Delta U}{\sqrt{g\beta\Delta S l_i}\sqrt{R_\rho - 1}} = \frac{\kappa_T \Delta U^3(\sqrt{R_\rho} - \sqrt{R_\rho - 1})^2}{16 Fr_c^2 \nu^{3/2} g\beta\Delta S(R_\rho - 1)^2}, \tag{23}$$

is also very sensitive to ΔU. The salt-flux

$$g\beta\langle F_S\rangle = \left(\frac{1}{2\sigma t_{\max}}\right)\frac{Fr_c^2 \nu(\kappa_T - R_\rho\kappa_S)^{1/2}(g\beta\Delta S)^2(R_\rho - 1)^{3/2}}{\kappa_T^{1/2}\Delta U^2(\sqrt{R_\rho} - \sqrt{R_\rho - 1})}, \tag{24}$$

provided the background shear U_z is strong enough to suppress square planform ($k_x = k_y$) fingers in favor of shear-aligned sheets ($k_x = 0$) and the fingers can grow to their maximum possible height (22). Predicted fluxes from (24) decrease rather than increase with ΔU and are much larger than Linden (1974) lab values (Figs. 5a and 6a). Associated with the large model fluxes are interface thicknesses much larger than the 0.1-m height of his tank ($l_i = h_{\max} > 5$ m, Figs. 5b and 6b) and very weak background Froude numbers ($U_z/N < 0.05$, Figs. 5c and 6a).

Figure 6a combines the laboratory fluxes from all six of Linden's runs and model fluxes as a function of background Froude number U_z/N using (21) and (22). The fluxes have been normalized by the unsheared fluxes. We caution that the horizontal axis is model dependent since Linden did not quote interface thicknesses; as shown below, U_z/N is likely underestimated in Figures 6a and b because the laboratory interfaces could not be as thick as the model predictions.

For $U_z/N < 0.1$, predicted fluxes are much larger than those observed (Fig. 6a). These large model fluxes correspond to extremely thick model interfaces at low U_z/N

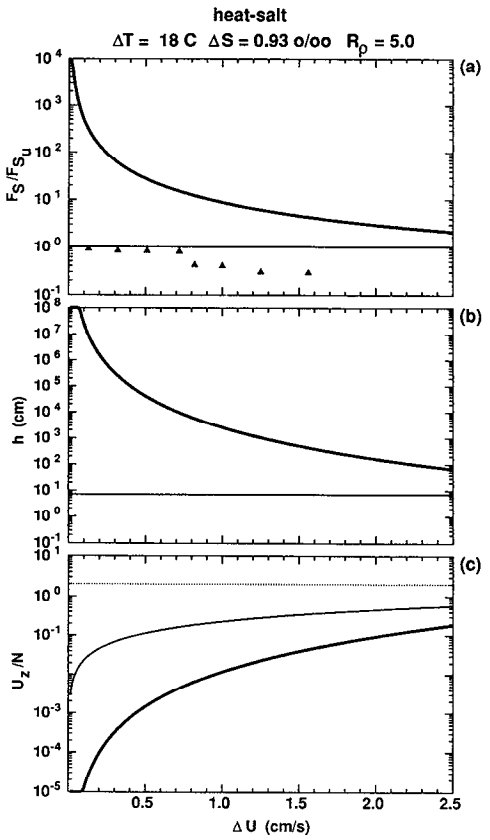

Figure 5. Model and laboratory salt-fluxes (a), maximum finger height $h_{max} = l_i$ (b) and background Froude number U_z/N (c) as functions of velocity step ΔU. The salt-fluxes have been normalized by the unsheared flux F_{S_u}. Laboratory fluxes (▲) are from one of Linden's (1974) heat-salt runs. Model values are for shear-aligned salt sheets (thick solid) and unsheared square planform fingers (thin solid) using the laboratory values of $\Delta T = 18°C$, $\Delta S = 0.93$ ‰ and $R_\rho = 5.0$ and assume the interface thickness is equal to the maximum finger height ($l_i = h_{max}$).

(Fig. 6b) because of the sensitivity of $l_i = h_{max}$ to ΔU in (22). Overestimated $l_i = h_{max}$ implies underestimated U_z/N from (23) and overestimated model salt-fluxes F_S from (24).

Linden (1974) reported that his splitter-plate configuration did not allow heat-salt fingers to grow to their full marginally-stable height. This 'shadowing' effect is evident in the heat-salt runs (▲) as U_z/N increases (Fig. 6a and c). Given the limitations on interface thickness imposed by Linden's 0.1-m tank height, his sheared fingers could not grow much taller than unsheared square planform fingers in any case. Figures 6c and 6d explore the consequences of this by applying unsheared constraint (17). The largest effect is to limit the range of the background Froude

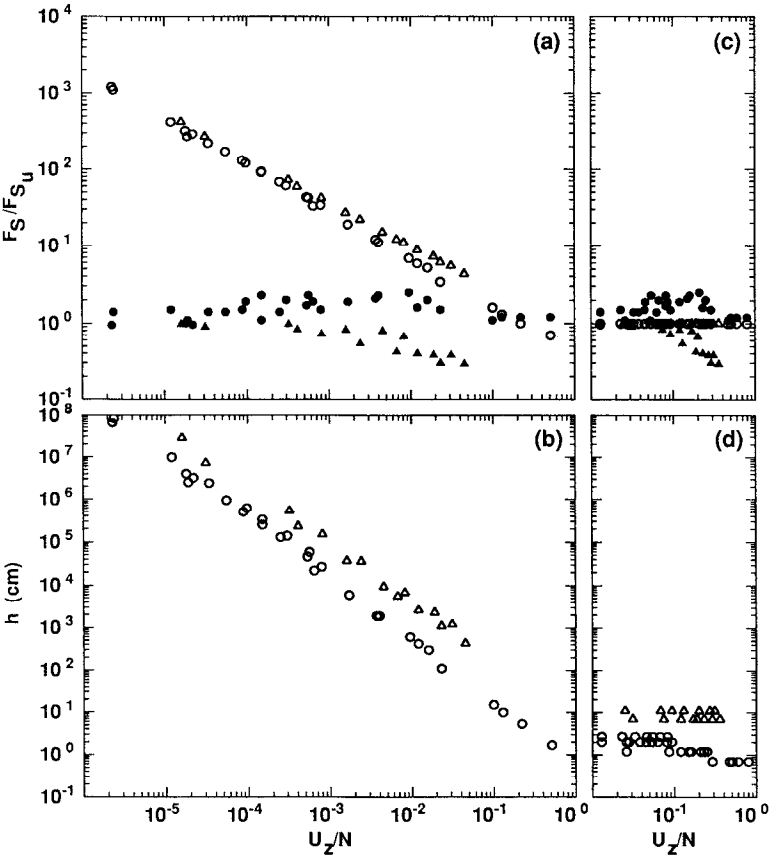

Figure 6. Model and laboratory (Linden, 1974) salt-fluxes (upper panels) and maximum finger heights $h_{max} = l_i$ (lower panels) as functions of background Froude number U_z/N. Left panels display shear-aligned sheet values (22)–(24) and the right panels unsheared square planform finger values (17). Model results are indicated by open symbols, lab values by closed symbols. Salt-fluxes (upper panels) are normalized by the unsheared fluxes for the same $\alpha\Delta T$ and $\beta\Delta S$ with sugar-salt runs indicated by circles and heat-salt runs by triangles. Sheet model fluxes (a) greatly exceed the lab fluxes for $U_z/N \ll 0.1$ with shadowing effects evident in the heat-salt runs (Δ) as U_z/N increases. For $U_z/N < 0.1$, shear-aligned sheets (b) exceed the height of the tank.

number U_z/N to 0.01–1.0 by restricting the interface thickness $l_i = h_{max}$ to 1–10 cm (Fig. 6d). The model fluxes are in closer agreement with the laboratory values, indicating that either (i) constraint (15) is invalid for $U_z/N < 0.1$ and constraints (16) or (17) more appropriate, or (ii) the lab configuration prevented realization of marginally-stable sheared sheets. In support of the first possibility, back-of-the-envelope calculations reveal that shear-tilting will be unable to suppress alongshear finger-induced microstructure for $U_z/N < 0.01$. Unfortunately, Linden measured

neither the interface thickness nor alongshear microstructure, so the reasons for the discrepancy between the model and lab values cannot be determined.

6. Discussion

The arguments leading to the proposed hybrid wave/finger Froude number constraint (15) have been entirely heuristic. The sole support for this constraint comes from its reproducing the dependence of Cox number on interface thickness reported by Marmorino (1989) and Fleury and Lueck (1991) for background Froude numbers $|\mathbf{V}_z|N = U_z/N = 0.1$–$1.0$. The model is unable to reproduce the laboratory measurements of Linden (1974) but whether this is due to failure of the model or limitations of his splitter-tank approach could not be determined without knowing the interface thickness l_i, and the vertical, along- and across-shear finger-induced microstructure. Nonetheless, the oceanic comparison should be encouraging enough to warrant further investigation.

a. In the limit as $|\mathbf{V}_z|/N \to 0$. As the background Froude number U_z/N approaches zero, constraint (15) indicates unbounded fluxes. This is clearly unrealistic. There must be a transition to square planform ($k_x = k_y$) fingers (17) via (16) as the background shear weakens. As this occurs, the Cox number should become independent of temperature gradient as in Kunze (1987). Since this does not occur in the range spanned by the C-SALT data (Fig. 3), shear-aligned sheets ($k_x = 0$) appear to dominate fluxes for wave Froude numbers $U_z/N \geq 0.1$ (Fig. 2). This is an exceptionally low finescale Froude number for the ocean where 1-m $|\mathbf{V}_z|/N > 0.1$ and usually > 0.5 (e.g., Kunze *et al.,* 1990; Pinkel and Anderson, 1994); infinitesimal shears ($|V_z|/N \ll 0.1$) do not exist in the ocean because of the omnipresence of internal waves. This suggests that sheets and constraint (15) may always apply in the ocean.

However, the transition from shear-aligned sheets to square planform fingers as $U_z/N \to 0$ may be important for understanding the model's discrepancy with Linden's laboratory fluxes (Fig. 5a) where background Froude numbers U_z/N may fall below 0.1 (Fig. 6).

b. Testing in the laboratory or numerically. To test predictions (22), (23) and (24) in the lab or numerically, a series of two-layer rundown heat-salt or sugar-salt experiments with varying ΔU could be performed. This promises to be challenging given the extreme sensitivity to ΔU and $Fr_{w/f}$ in (23) and (24). Measurements of interface thickness l_i, interfacial vertical shear U_z, and vertical, along- and across-shear microstructure (e.g., Taylor and Bucens, 1989) as well as $\alpha\Delta T$, $\beta\Delta S$, ΔU and fluxes would be needed to establish (i) whether laboratory setups are reproducing appropriate conditions to test the above predictions (e.g., no alongshear finger-induced microstructure), (ii) at what U_z/N square planform fingers are suppressed in favor of shear-aligned sheets [since tilted fingers viewed from above as by Linden (1974)

might look like sheets], and (iii) test (15) if alongshear finger-induced microstructure is suppressed and (16) if it is not. Initiating sheared experiments with thin interfaces also raises the danger of shear instability playing a role in thickening them at the outset (9). This could be alleviated by starting with thicker interfaces.

Care must be taken to avoid the shadow effects reported by Linden (1974) which prevent fingers from growing to their full marginally-stable height. Shadowing might be eliminated by using a racetrack tank with no obstacles around its circumference (e.g., Ruddick *et al.,* 1989), although flow curvature could introduce other problems. If using a rotating tank and geostrophic shear, care must be taken that the inertial frequency $f = 2\Omega$ is much less that the finger growth rate σ so that rotation does not affect the fingers (Schmitt and Lambert, 1979).

With recent advances allowing numerical simulations to handle high Prandtl number $\nu/\kappa_T \gg 1$ and low diffusivity ratio $\kappa_S/\kappa_T \ll 1$ convection accurately (Shen, 1993), numerical modelling might be a more practical way of testing the proposed constraint. Shadowing could be eliminated by using a horizontally-periodic domain in the alongshear direction. However, the vertical extent of the domain must be large enough to include one interface thickness l_i (Fig. 5b). This may restrict simulations to $U_z/N > 0.1$ (Figs. 5b and 6b) unless square planform fingers dominate at low shears.

c. Oceanic consequences. What are the implications of the suggested constraint in the main pycnocline? Following Schmitt (1981) by taking S_{z_o} to be the largescale gradient smoothed over the staircase rather than the finescale interface gradients experienced by fingers, $\overline{S}_z$, the finger-induced eddy diffusivity for salt can be expressed

$$K_{Sf} = \frac{F_S}{S_{z_o}} = \frac{\langle w\delta S\rangle}{S_{z_o}} = \frac{\langle wh\rangle}{4}\frac{l_o + l_i}{l_i} = \frac{\sigma\langle h^2\rangle}{8}\frac{l_o + l_i}{l_i}, \tag{25}$$

where l_o and l_i are the layer and interface thicknesses (for a smoothly-stratified fluid, the layer thickness $l_o = 0$ and the largescale gradient S_{z_o} is identical to the gradient felt by the fingers $\overline{S}_z$).

For $Fr_c = U_z k w/N^2 = U_z k\sigma h_{\max}/2N^2 = 1.0$, it follows that $h^2_{\max} = 4N^4/U_z^2k^2\sigma^2$ and the eddy diffusivity (25) becomes

$$\boxed{K_{Sf} \simeq \frac{\nu}{Fr_w^2}\frac{\sqrt{R_\rho - 1}}{\sqrt{R_\rho} - \sqrt{R_\rho - 1}}\frac{l_o + l_i}{l_i}} \tag{26}$$

depending inversely on the wave Froude number squared (or linearly on the wave Richardson number) for shear-aligned sheets ($Fr_w > 0.1$). Below we describe the finger-induced salt diffusivity for typical smoothly-stratified, $Fr_w = 1.0$ conditions, then explore the impact of intermittent turbulence, weaker background shear and finally staircase conditions.

In most of the upper ocean, organized staircases are absent and internal-wave Froude numbers $Fr_w \simeq 1.0$ due to near-inertial waves (Simpson *et al.,* 1979; Evans, 1981; Kunze *et al.,* 1990; Pinkel and Anderson, 1994). For these typical upper-ocean conditions, (26) reduces to

$$K_{Sf} \simeq \nu \frac{\sqrt{R_\rho - 1}}{\sqrt{R_\rho} - \sqrt{R_\rho - 1}} \tag{27}$$

(thick solid curve in Fig. 7) as in unsheared, square planform fingers (Kunze, 1987). The salt diffusivity (27) is just the molecular viscosity times a function of density ratio. It is at most a few times 0.01×10^{-4} m^2 s^{-1} as compared to typical turbulent eddy diffusivities of $0.05–0.15 \times 10^{-4}$ m^2 s^{-1} (Gregg, 1989; Polzin *et al.,* 1994; Ledwell *et al.,* 1993; Toole, *et al.,* 1994).

Counterintuitively, the diffusivities in (27) are weakest as $R_\rho \to 1$, that is, for the most destabilizing density ratio. This is because, for a given $\overline{S}_z$, lower density ratios imply weaker stabilizing stratifications $N^2 = g\beta\overline{S}_z(R_\rho - 1)$. However, growth rates are slower at higher density ratios, making fingers more susceptible to disruption by shear-generated turbulence. Linden (1971) showed that even weak turbulence [$\epsilon > \sim O(10^{-10}\ W\ \mathrm{kg}^{-1})$] completely quenched finger fluxes. Crudely, turbulence is present in the pycnocline about 10% of the time, arising roughly every ten buoyancy periods (though this must be considered speculative as there are no truly Lagrangian time-series of turbulent properties). Thus, fingers requiring more than ten buoyancy periods to achieve $Fr_{w/f} \geq 1$ should be disrupted by turbulence rather than self-instability, and so will have diffusivities diminished from (25). For $Fr_w = 1.0$ and following Kunze (1987), this reduces finger fluxes at density ratios $R_\rho > 2$ (dotted curve in Fig. 7). Since the growth rate of salt sheets is unaffected by the shear magnitude, this curve is independent of U_z/N—or would be if U_z/N didn't affect the frequency of occurrence of turbulent events. Turbulence was weaker and less frequent (1%) in the staircase east of Barbados where $U_z/N \simeq 0.4$ (Gregg and Sanford, 1987; Marmorino, 1990; Fleury and Lueck, 1991).

Provided the background shear is strong enough to suppress alongshear structure ($U_z/N > 0.1$), salt-finger fluxes are enhanced in weaker background shear (19) because smaller U_z/N allows larger w_y/N by suppressing w_x/N. In the staircase east of Barbados ($Fr_w \sim 0.4$, Gregg and Sanford, 1987), the fluxes (thin dashed curve in Fig. 7) are a factor of six larger than for planform fingers ($U_z = 0$, $w_x = w_y$) constrained by the finger Froude number $|\nabla w|/N \leq 1.0$ or $|w_x w_y|/N^2 \leq 1.0$.

Staircase structure also enhances the fluxes (26) by introducing strong interfacial gradients (thick dashed curve in Fig. 7). Salt-fingering diffusivities are an order of magnitude stronger in the thermohaline staircase east of Barbados than they would be in a smoothly-stratified pycnocline. This emphasizes that staircases are sites of augmented finger fluxes. Persistent staircases are only observed in the ocean for density ratios $R_\rho \leq 1.7$ (Schmitt, 1994).

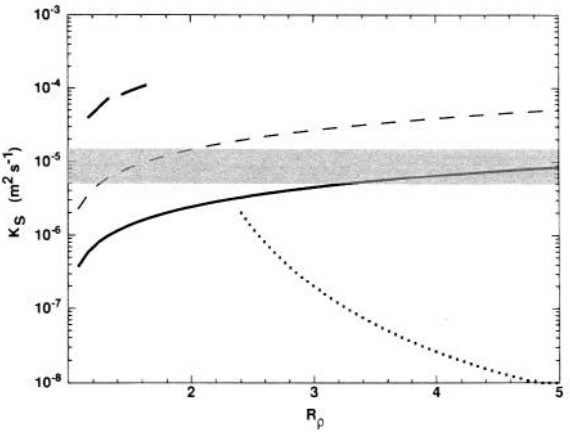

Figure 7. Model finger salinity diffusivity K_S as a function of density ratio R_ρ. For continuously-stratified conditions for a wave Froude number $Fr_w = 1.0$ (thick solid) and $Fr_w = 0.4$ (thin dashed), higher diffusivities occur at higher density ratios. If finger growth is disrupted by turbulence every ten buoyancy periods, the finger diffusivity is depressed for density ratios $R_\rho > 2$ (dotted curve). In thermohaline staircases (found only for $R_\rho < 1.7$) such as the one east of Barbados where the layer thickness l_o is ten times the interface thickness l_i the diffusivity is boosted (thick dash). The band of stippling shows the typical range of turbulent diffusivities in the pycnocline (Gregg, 1989; Ledwell *et al.*, 1993; Polzin *et al.*, 1994).

The ocean seems best described by weakly-sheared staircases for density ratios $R_\rho < 1.7$ (thick dash, Fig. 7) and finger fluxes disrupted by turbulence rather than self-instability for $R_\rho > 2$ (thick dotted). The shape of the resulting dependence of finger diffusivity on density ratio, with dramatically-elevated fluxes for $R_\rho < 1.7$ because of staircase layering, is remarkably similar to that inferred by Schmitt (1981, his Fig. 5), albeit one to two orders of magnitude weaker.

Kunze (1987) pointed out that the C-SALT interfaces are an order of magnitude too thick to support laboratory $\Delta S^{4/3}$ fluxes. If the assumption that $l_i = h_{\max}$ (21) is naively applied to typical C-SALT interface thicknesses of $l_i = 3$ m, it implies velocity steps $\Delta U = 0.12$ cm s^{-1}, much smaller than those observed (Fig. 2), and background Froude numbers, $U_z/N = 0.03$. Thus, the constraint proposed here cannot explain the interface thicknesses either.

The intermittent occurrence of shear-generated turbulence may prevent ocean interfaces from sharpening like those in the lab (Stern and Turner, 1969). For a given internal-wave interfacial velocity step ΔU, if an interface sharpens, the wave Froude number will increase (Fig. 2b), increasing the frequency of occurrence and strength of shear-driven turbulent mixing which will diffuse the interface. Likewise, shear-generated turbulence will weaken as the interface thickens, allowing finger fluxes to sharpen the gradients. Thus, shear-driven turbulence acting in opposition to the double-diffusive tendency to sharpen interface gradients may explain why ocean interfaces remain too thick to support laboratory $\Delta S^{4/3}$ fluxes. Walsh and Ruddick (1994) show that the dependence of the diffusivity on density ratio effects the

stability of small interleaving perturbations with eddy diffusivity K increasing with R_ρ producing growing instability. This mechanism too could lead to staircase formation and maintenance.

d. Summary. This paper sought a constraint for salt-finger growth in shear that would explain the observed Cox numbers' dependence on temperature gradient in C-SALT (Marmorino, 1989; Fleury and Lueck, 1991). While the proposed constraint (15) reproduces the oceanic observations for $U_z/N > 0.1$, its predictions were not consistent with the results of Linden's (1974) two-layer laboratory experiments. There are many possible reasons for this discrepancy. Chief among them are that constraint (15) is wrong, and (22)–(24) display extreme sensitivity to ΔU; Linden's experimental configuration might not have allowed shear-aligned sheets to grow to their full marginally-unstable heights, may have had shears too weak to suppress square planform fingers in favor of shear-aligned sheets, or may have been influenced by shear-induced turbulence at the outset. Shears $U_z/N < 0.01$ will be too weak to suppress alongshear finger-induced microstructure so that the more generalized constraint (16) should be applied; for very weak background shears $U_z/N \ll 1.0$, (16) is well-approximated by (17). Oceanic Froude numbers always exceed 0.1 because of the omnipresence of finescale internal waves.

Acknowledgments. Mike Gregg is thanked for sharing the MSP velocity data from C-SALT and for pointing out a factor-of-two error in the time-integral normalization in Kunze (1987). Insightful comments were provided by two anonymous reviewers, George Marmorino, Barry Ruddick, David Walsh, Ray Schmitt and Dan Kelley. This work was supported under NSF grant OCE-92-404-93.

REFERENCES

Boyd, J. D. and H. Perkins. 1987. Characteristics of thermohaline steps off the northwest coast of South America. Deep-Sea Res., *34,* 337–364.

Evans, D. L. 1981. Velocity shear in a thermohaline staircase. Deep-Sea Res., *28A,* 1409–1415.

Fleury, M. and R. G. Lueck. 1991. Fluxes across a thermohaline interface. Deep-Sea Res., *38,* 745–769.

Gargett, A. E. and R. W. Schmitt. 1982. Observations of salt fingers in the Central Waters of the eastern North Pacific. J. Geophys. Res., *87,* 8017–8029.

Gregg, M. C. 1989. Scaling turbulent dissipation in the thermocline. J. Geophys. Res., *94,* 9686–9698.

Gregg, M. C. and T. B. Sanford. 1987. Shear and turbulence in thermohaline staircases. Deep-Sea Res., *34,* 1689–1696.

Kunze, E. 1987. Limits on growing, finite-length fingers: A Richardson number constraint. J. Mar. Res., *45,* 533–556.

—— 1990. The evolution of salt fingers in inertial wave shear. J. Mar. Res., *48,* 471–504.

Kunze, E., A. J. Williams III and M. G. Briscoe. 1990. Observations of shear and vertical stability from a neutrally-buoyant float. J. Geophys. Res., *95,* 18,127–18,142.

Kunze, E., A. J. Williams III and R. W. Schmitt. 1987. Optical microstructure in the thermohaline staircase east of Barbados. Deep-Sea Res., *34,* 1697–1704.

Lambert, R. B. and W. Sturges. 1977. A thermohaline staircase and vertical mixing in the thermocline. Deep-Sea Res., *24,* 211–222.

Ledwell, J. R., A. J. Watson and C. S. Law. 1993. Evidence of slow mixing across the pycnocline from an open-ocean tracer-release experiment. Nature, *364,* 701–703.

Linden, P. F. 1971. Salt fingers in the presence of grid-generated turbulence. J. Fluid Mech., *49,* 611–624.

—— 1973. On the structure of salt fingers. Deep-Sea Res., *20,* 325–340.

—— 1974. Salt fingers in a steady shear flow. Geophys. Fluid Dyn., *6,* 1–27.

Lueck, R. G. 1987. Microstructure measurements in a thermohaline staircase. Deep-Sea Res., *34,* 1677–1688.

Marmorino, G. O. 1989. Substructure of oceanic salt finger interfaces. J. Geophys. Res., *94,* 4891–4904.

—— 1990. "Turbulent mixing" in a salt-finger interface. J. Geophys. Res., *95,* 12,983–12,994.

Pinkel, R. and S. Anderson. 1994. Richardson number statistics and internal wave breaking. EOS Transac., *75(3),* 120.

Polzin, K., J. M. Toole and R. W. Schmitt. 1994. Finescale parameterizations of turbulent dissipation. J. Phys. Oceanogr. (submitted).

Ruddick, B. R., R. W. Griffiths and G. Symonds. 1989. Frictional stress at a sheared double-diffusive interface. J. Geophys. Res., *94,* 18,161–18,174.

Schmitt, R. W. 1979. Flux measurements at an interface. J. Mar. Res., *37,* 419–436.

—— 1981. Form of the temperature-salinity relationship in the Central Water: Evidence for double-diffusive mixing. J. Phys. Oceanogr., *11,* 1015–1026.

—— 1994. Double diffusion in oceanography. Ann. Rev. Fluid Mech., *26,* 255–285.

Schmitt, R. W. and R. B. Lambert. 1979. The effects of rotation on salt fingers. J. Fluid Mech., *90,* 449–463.

Schmitt, R. W., H. Perkins, J. D. Boyd and M. C. Stalcup. 1987. C-SALT: An investigation of the thermohaline staircase in the western tropical North Atlantic. Deep-Sea Res., *34,* 1655–1666.

Shen, C. Y. 1993. Heat-salt finger fluxes across a density interface. Phys. Fluids, *A5,* 2633–2643.

Shirtcliffe, T. G. L. and J. S. Turner. 1970. Observations of the cell structure of salt fingers. J. Fluid Mech., *41,* 707–719.

Simpson, J. H., M. R. Howe, N. C. G. Morris and J. Stratford. 1979. Velocity shear on the steps below the Mediterranean outflow. Deep-Sea Res., *26A,* 1381–1386.

Stern, M. E. 1969. Collective instability of salt fingers. J. Fluid Mech., *35,* 209–218.

—— 1975. Ocean Circulation Physics. Academic Press, NY, 191–203.

Stern, M. E. and J. S. Turner. 1969. Salt-fingers and convecting layers. Deep-Sea Res., *16,* 497–511.

Taylor, J. and P. Bucens. 1989. Laboratory experiments on the structure of salt fingers. Deep-Sea Res., *36,* 1675–1704.

Toole, J. M., K. L. Polzin and R. W. Schmitt. 1994. Estimates of diapycnal mixing in the abyssal ocean. Science, *264,* 1120–1123.

Turner, J. S. 1967. Salt fingers across a density interface. Deep-Sea Res., *14,* 599–611.

Walsh, D. and B. Ruddick. 1994. An investigation of Kunze's salt-finger flux laws—Are they stable? Proc. AGU Chapman Conference on Double-Diffusive Convection, A. Brandt and J. Fernando, eds., (submitted).

Received: *15 December, 1993;* revised: *9 June, 1994.*